THE JOURNAL OF BIOLOGICAL CHEMISTRY
Vol. 276, No. 22, Issue of June 1, pp. 18795–18803, 2001

*Printed in U.S.A.*

# Identification of Molecular Determinants That Are Important in the Assembly of *N*-Methyl-D-aspartate Receptors*

Received for publication, February 13, 2001, and in revised form, March 2, 2001
Published, JBC Papers in Press, March 6, 2001, DOI 10.1074/jbc.M101382200

**Elisabeth Meddows‡§¶, Béatrice Le Bourdellès§, Sarah Grimwood§, Keith Wafford§, Satpal Sandhu§, Paul Whiting§, and R. A. Jeffrey McIlhinney‡‖**

*From the ‡Medical Research Council Anatomical Neuropharmacology Unit, Mansfield Road, Oxford OX1 3TH and the §Neuroscience Research Centre, Merck Sharp & Dohme, Terlings Park, Eastwick Road, Harlow, Essex CM20 2QR, United Kingdom*

**To determine which domains of the *N*-methyl-D-aspartate (NMDA) receptor are important for the assembly of functional receptors, a number of N- and C-terminal truncations of the NR1a subunit have been produced. Truncations containing a complete ligand binding domain bound glycine antagonist and gave binding constants similar to those of the native subunit, suggesting they were folding to form antagonist binding sites. Since NR2A is not transported to the cell surface unless it is associated with NR1 (McIlhinney, R. A. J., Le Bourdellès, B., Tricuad, N., Molnar, E., Streit, P., and Whiting, P. J. (1998) *Neuropharmacology* 37, 1355–1367), surface expression of NR2A can be used to monitor the association of the subunits. There was progressive loss of NR2A cell surface expression as the N terminus of NR1a was shortened, with complete loss when truncated beyond residue 380. Removal of the C terminus and/or the last transmembrane domain did not affect NR2A surface expression. Similar results were obtained in co-immunoprecipitation experiments. The oligomerization status of the co-expressed NR1a constructs and NR2A subunits was investigated using a non-denaturing gel electrophoresis system (blue native-polyacrylamide gel electrophoresis) and sucrose density gradient centrifugation. The blue native-polyacrylamide gel electrophoresis system also showed that the NR1a subunits could form a homodimer, which was confirmed using soluble constructs of the NR1a subunit. Together these results suggest the residues N-terminal of residue 380 are important for the association of NR2A with NR1a and that the complete N-terminal domain of the NR1a subunit is required for oligomerization with NR2A.**

The *N*-methyl-D-aspartate (NMDA)[1] subtype of the glutamate receptor family is a hetero-oligomeric protein composed of two classes of NMDA receptor subunits: NR1 and NR2. The NR1 subunit is encoded by a single gene, which undergoes extensive splicing to generate eight different splice variants that differ in regional distribution and functional properties (2). The NR2 subunit class consists of four different subunits, NR2A–NR2D, encoded by four separate but closely related genes (2). A number of studies of mammalian cell lines either permanently or transiently transfected with NR1 alone have indicated that the NR1 subunit does not form glycine-glutamate-responsive channels and requires the presence of NR2 to do so (3–5). Other studies have shown that the NR1 and NR2 subunits contribute differently to the binding sites of a functional NMDA receptor. The NR1 subunit forms the glycine binding site (6–8), and the NR2 subunit provides part of the glutamate binding site (9, 10). Thus, different combinations of both subunits co-assemble to form functionally distinct NMDA receptors. However, the biochemical and functional studies reported to date are ambiguous with regard to NMDA receptor subunit stoichiometry. Functional studies indicate that binding of at least two molecules of both glutamate and glycine is required for NMDA receptor activation, suggesting that at least four subunits must co-assemble (11–13). The molecular size of native NMDA receptors, as determined by both gel filtration and native polyacrylamide gel electrophoresis, is in the range of 605–850 kDa, which is consistent with the co-assembly of between four to five subunits (14–16). A recent biochemical study has suggested that there are three NR2 subunits per NMDA receptor complex, indicating that the NMDA receptor is at least a pentamer (17). Electrophysiological studies on the subunit stoichiometry using co-expressed wild-type and mutant forms of either the NR1 or NR2 subunits have also been inconclusive suggesting two or three NR1 subunits or two or three NR2 subunits per functional NMDA receptor complex (18–20).

The regions of NMDA receptor subunits mediating the assembly of hetero-oligomeric NMDA receptors have, to date, not been identified. All glutamate receptor subunits are thought to share a common transmembrane topology and domain structure with three transmembrane domains (TMI, -III, and -IV), a second membrane domain forming a re-entrant loop that partly lines the ion channel pore, an extracellular N terminus, and an intracellular C terminus (21–23). The ligand binding domain is thought to be formed between part of the N terminus (the S1 domain) just before TMI and the extracellular loop between TMIII and TMIV (the S2 domain) (6, 24, 25). Approximately the first 400 amino acids of the N terminus share sequence homology to the bacterial periplasmic leucine-isoleucine-valine-binding protein (LIVBP domain) (26). The proximal N-terminal domain has recently been suggested to be important in the assembly of AMPA receptor subunits in mammalian cells (27).

In this study we addressed the question of which domains of the NR1a NMDA receptor subunit are important for their

* The costs of publication of this article were defrayed in part by the payment of page charges. This article must therefore be hereby marked "*advertisement*" in accordance with 18 U.S.C. Section 1734 solely to indicate this fact.

¶ Supported by a Medical Research Council Industrial Collaborative Studentship.

‖ To whom correspondence should be addressed. Tel.: 44-01865-271896; Fax: 44-01865-271647; E-mail: jeff.mcilhinney@pharm.ox.ac.uk.

[1] The abbreviations used are: NMDA, *N*-methyl-D-aspartate; TM, transmembrane domain; nAChR, nicotinic acetylcholine receptor; HEK, human embryonic kidney; PAGE, polyacrylamide gel electrophoresis; BN, blue native; AMPA, α-amino-3-hydroxy-5-methyl-4-isoxazole proprionate; BisTris, bis(2-hydroxyethyl)iminotris(hydroxymethyl)methane; $GABA_A$, γ-aminobutyric acid subunit A.

assembly into oligomeric receptor complexes. Human embryonic kidney (HEK) 293 cells were transfected with mutated NR1a constructs containing deletions to the N and C termini, NR1a chimeras, and soluble secreted forms of the NR1a subunit and wild-type NR2A subunits. Since we have shown previously that NR2A is not expressed at the cell surface unless it is co-expressed with NR1 (1), cell surface expression of the NR2A subunit has been used to monitor subunit association, together with co-immunoprecipitation of the different subunits. The formation of oligomeric complexes has been monitored using a novel nondenaturing gel electrophoresis system and sucrose gradient sedimentation.

## EXPERIMENTAL PROCEDURES

*Design of the NR1a Truncations*—All the truncated NR1a subunits are derived from a human NR1a cDNA and were generated by using standard mutagenesis techniques previously described in detail (28). An octapeptide FLAG epitope tag (KDYKDDDDK) was introduced into the N terminus between $Asp^{23}$ and $Lys^{25}$, just C-terminal to the putative signal cleavage point. The constructs were verified by sequencing and by *in vitro* translation (TNT T7 Transcription/Translation System; Promega; Fig. 1). Radioligand binding assays using [$^3$H]L-689,560 were performed as previously described in detail (4, 28).

*Transfection of HEK-293 Cells*—HEK-293 cells were cultured and transfected using the calcium phosphate method. The NMDA receptor NR1a and NR2A subunits in the expression vectors pcDNAI/Amp and pCDM8 were transfected at a ratio of 1:3. After transfection, the cells were grown in the presence of 0.5 mM ketamine (Sigma) and harvested 24 h later. Membranes were prepared from the cells using hypotonic lysis, shearing, and centrifugation as described previously (29) except that 20 mM iodoacetamide was added to the lysis medium prior to cell lysis.

*Expression in Xenopus Oocytes and Electrophysiological Recordings*—Adult female *Xenopus laevis* were anesthetized by immersion in a 0.1% solution of 3-aminobenzoic acid ethyl ester, with the pH adjusted with 1 M $NaHCO_3$ to that of the water in which the toad was housed, for 30–45 min, and stage V and stage VI oocytes were surgically removed. After mild collagenase treatment to remove follicle cells (type IA, 0.5 mg/ml, for 6 min), the oocyte nuclei were directly injected with 10–20 nl of injection buffer (88 mM NaCl, 1 mM KCl, 15 mM HEPES, at pH 7, filtered through nitrocellulose) containing different combinations of human NMDA subunit cDNAs (20 ng/$\mu$l) engineered into the expression vector pCDM8 or pcDNAI/Amp. NR1a truncations and NR2A cDNAs were injected at a ratio of 1:3. Oocytes were maintained at 19–20 °C in modified Barth's medium consisting of 88 mM NaCl, 1 mM KCl, 10 mM HEPES, 0.82 mM $MgSO_4$, 0.33 mM $Ca(NO_3)_2$, 0.91 mM $CaCl_2$, 2.4 mM $NaHCO_3$, at pH 7.5 supplemented with 50 $\mu$g/ml gentamycin, 10 $\mu$g/ml streptomycin, 10 units/ml penicillin, and 2 mM sodium pyruvate) for up to 6 days. For electrophysiological recordings, oocytes were placed in a 50-$\mu$l bath and continually perfused at 4–6 ml/min with Barium Ringer's solution (115 mM NaCl, 2.5 mM KCl, 10 mM HEPES, 1.8 mM $BaCl_2$, pH 7.2). Cells were impaled with two 1–3-megohm electrodes containing 2 M KCl and voltage-clamped at −70 mV. In all experiments drugs were applied in the perfusate until the peak of the response was observed.

*Cell Surface Biotinylation*—Transiently transfected HEK-293 cells were overlaid with borate buffer (10 mM boric acid, 150 mM NaCl, pH 8.8) containing 50 $\mu$g/ml of the non-permeant reactive ester sulfo-NHS-biotin (Pierce; dissolved at 10 mg/ml in *N,N*-dimethylformamide). Unreacted ester was removed by incubating the cells for 5 min with 1 M ammonium chloride. The cells were washed with Tris-saline (pH 7.4) then lysed on ice in RIPA buffer (50 mM Tris-HCl, pH 7.5, 1% (w/v) Triton X-100, 0.5% sodium deoxycholate, 0.1% SDS, 100 mM NaCl, 1 mM EDTA) plus a protease inhibitor mixture (Roche Molecular Biochemicals) and 20 mM iodoacetamide. The lysate was centrifuged at 10,000 × *g*, and a tenth of the supernatant removed for total cell lysate analysis. The biotin-labeled surface proteins in the remaining supernatants were affinity isolated with 100 $\mu$l of streptavidin-agarose beads (Sigma) rotating for 3.5 h at 4 °C. The resulting pellets were washed twice with RIPA buffer and twice with 50 mM Tris-HCl, pH 8.0, and proteins eluted from the streptavidin-agarose beads by addition of 2× reducing sample buffer (20 mM dithiothreitol, 2% (w/v) SDS, 10% (v/v) glycerol, 100 mM Tris-HCl). The samples were then analyzed using SDS-PAGE and the Western immunoblot protocol. The possibility that the sulfo-NHS-biotin penetrates the cells during the biotinylation procedure was controlled for by probing the total cell lysates and streptavidin isolates for the intracellular protein $\beta$-tubulin. Only those experiments in which this control was negative were used for analysis.

*Co-immunoprecipitation*—Transiently transfected HEK-293 cells were lysed on ice with RIPA buffer containing 20 mM iodoacetamide and protease inhibitors (Roche Molecular Biochemicals). The lysate was centrifuged at 10,000 × *g*, and an aliquot was removed for total cell lysate analysis. A fifth of the lysate was made up to 1 ml with lysis buffer and then rotated overnight at 4 °C with 1–2 $\mu$g/ml precipitating antibody. A 100-$\mu$l suspension of Protein G-Sepharose Fast Flow beads (Amersham Pharmacia Biotech) was added to the precipitates and mixed by rotation at 4 °C for 2 h. The immunoprecipitates were pelleted by centrifugation, and the resulting pellet was washed twice in RIPA buffer and then twice with 50 mM Tris-HCl, pH 8.0. Under these conditions, quantitative immunoprecipitation of the subunits was achieved. The immunocomplexes were eluted from the Protein G beads by mixing with 2× reducing sample buffer and boiling the samples. Both the precipitates and total cell lysates were resolved by SDS-PAGE and Western immunoblot. The antibodies used for immunoprecipitation were a sheep anti-NR1a antibody (previously characterized; Ref. 1) and the anti-FLAG antibody M2 from Sigma. The NR1-GluR1 chimera was precipitated using an anti-GluR1 antibody (30).

*Western Immunoblotting*—Proteins were separated by SDS-PAGE using 7.5% polyacrylamide gels under reducing conditions. After transfer to nitrocellulose membrane using a Transblot semidry transfer cell (Bio-Rad), the membranes were blocked in 5% (w/v) nonfat dried milk in phosphate-buffered saline plus 0.05% Tween for 1 h. The primary antibodies, applied to the immunoblots overnight at 4 °C, were a rabbit anti-NR2A antibody and the 23.F6 antibody, which recognizes the N terminus of NR2A (1). The NR1 subunit was detected using antibodies directed to residues 600–800 (NMDAR1; PharMingen) or to residues 1–564 of the subunit (Calbiochem) or the C-terminal tail. The primary antibodies were detected using the donkey anti-sheep (Sigma; 1/2000), goat anti-rabbit, or goat anti-mouse (Promega; 1/5000) antibodies conjugated to horseradish peroxidase in conjunction with the chemiluminescence SuperSignal kit (Pierce).

*Blue Native-PAGE (BN-PAGE)*—Analysis of the oligomeric structure of native protein complexes was achieved by using a modification of the method of BN-PAGE as described previously (31, 32). Membrane samples were prepared by mixing with 1 mg/ml DNase (+10 mM $CaCl_2$, 10 mM $MgCl_2$) and leaving at room temperature for 15 min. An equal volume of 2× BN-PAGE sample buffer (200 mM BisTris, 150 mM 6-aminocaproic acid, 2% Triton X-100, pH 7) was added to each sample and left on ice for 15 min. The membrane samples were centrifuged at 100,000 × *g* and mixed with 5% Serva blue dye. The markers thyroglobulin, bovine serum albumin, apoferritin, and $\beta$-amylase were mixed with 5% Serva blue dye and run with the samples on a 5–18% gel containing no detergent. The samples and markers were stacked at 100 V and then run at a constant 500 V (15 mA; 4 °C). The gel was then subjected to a revised Western immunoblot protocol. Excess dye from the top membrane was removed with destain (34% methanol, 10% acetic acid, 2% glycerol in $H_2O$). The marker lanes were stained with Coomassie Blue dye (50% methanol, 10% acetic acid, 0.2% (w/v) Coomassie Blue) and then destained to visualize the protein bands. The section of the membrane containing the proteins was washed with phosphate-buffered saline plus 0.05% Tween and processed in the same manner as the SDS-PAGE immunoblots. In order to calibrate the gel, membranes from cells expressing $GABA_A$ receptors of composition $\alpha_3\beta_3\gamma_2$ and purified *Torpedo* nACh receptors (nAChR) were used. The sera used for identification were anti-$\alpha$3 for the $GABA_A$ receptor and monoclonal antibody 210 (mAb210) for the nAChR, which recognizes an epitope on the $\alpha$1 subunit. These receptors and antibodies were generously provided by Merck Sharp & Dohme and Professor Lindstrom, University of Pennsylvania, respectively.

*Sucrose Density Gradient Centrifugation*—HEK-293 cell lysates were prepared by lysis in 1% (v/v) Triton X-100 in Tris-saline lysis buffer containing protease inhibitors and 20 mM iodoacetamide. Sucrose density centrifugation of HEK-293 cell lysates was performed using cell lysates layered on 4-ml continuous 10–40% (w/v) sucrose gradients centrifuged in a SW60 Sorvall rotor for 16 h at 100,000 × *g*, 4 °C. Twenty fractions were collected from each gradient and analyzed by SDS-PAGE.

*Chromatography of Soluble NR1a Subunits*—Five replicate 25-cm$^2$ flasks for each secreted protein were transfected with 10 $\mu$g of DNA. Fresh AimV medium (Life Technologies, Inc.), containing no serum and supplemented with 2 mM L-glutamine and 100 units/ml penicillin, was added 24 h after transfection, and the cells were left for another 3 days of growth. The medium, with added protease inhibitors, was centrifuged at 1000 × *g* for 10 min, the supernatant removed and concentrated down 5-fold using Vivaspin 4-ml concentration tubes. The concentrated medium was filtered and analyzed by chromatography on a

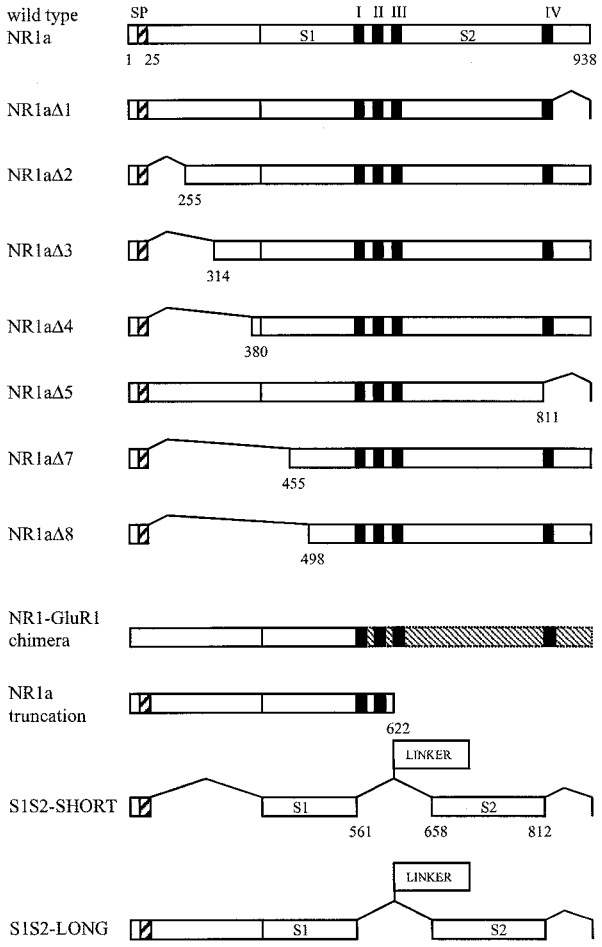


FIG. 1. **Truncations and chimeras of the human NR1a subunit.** The constructs NR1aΔ1-NR1aΔ8 were based on the wild-type human NR1a subunit and were generated by oligonucleotide-directed mutagenesis. The NR1a truncations are shown diagrammatically with the signal peptide (*SP*) and the transmembrane domains (*black boxes*) I–IV indicated. The position of each truncation is indicated by the residue number at the N or C terminus. The FLAG epitope was introduced into the constructs following the signal peptide as shown by the *cross-hatched box*. The truncated NR1a N terminus (NR1tr) terminates immediately after the putative re-entrant loop of the second membrane domain and the NR1-GluR1 chimera (R1ch) consists of the NR1a N terminus spliced to the GluR1 sequence (*hatched box*) just before TMI as illustrated. The soluble NR1a constructs, S1S2-LONG and S1S2-SHORT, were produced by site-directed mutagenesis techniques with the TMI-TMIII sequences, replaced by short oligonucleotide LINKER sequences encoding peptides of 28 amino acids.

Superose 6 column (Amersham Pharmacia Biotech) using a Liquid Chromatography Controller LCC-500. The fractions were analyzed by dot-blot, using nitrocellulose membrane (Schleicher & Schuell), and SDS-PAGE and both membranes processed using the Western immunoblot protocol.

## RESULTS

*Functional Expression of the NR1a Truncated Subunits*—The structures of the different NR1a constructs used in this study are illustrated in Fig. 1. All of the NR1a truncated subunits, with the exception of the NR1aΔ7, NR1aΔ8, the NR1a N-terminal truncation, and the NR1-GluR1 chimera, formed high affinity binding sites for the glycine antagonist [$^3$H]L-689,560 when expressed in HEK-293 cells (28). Since the NR1 truncations that did not bind the glycine antagonist contain deletions that remove parts of the S1 domain important for the formation of the glycine binding site, these results are in agreement with our current understanding of the structure of other glutamate receptor subunits.

HEK-293 cells co-expressing the NR1a constructs containing deletions up to residue 380 in the N terminus (NR1aΔ2-NR1aΔ4) and NR2A were analyzed for the expression of functional channels in *Xenopus* oocytes (Table I). Although unmodified NR1a and the NR1aΔ2 and NR1aΔ3 constructs formed functional channels with NR2A at the cell surface, deletion up to residue 380 within the N-terminal domain of NR1a (NR1aΔ4) abolished NMDA channel function (Table I). Similar data were also obtained in HEK-293 cells (data not shown). The currents found in the NR1aΔ2 and NR1aΔ3 constructs were reduced in amplitude compared with those seen with the wild-type NR1a and NR2A subunits, suggesting that these truncated subunits form smaller numbers of functional channels at the cell surface. Deletion of the C terminus (NR1aΔ1) and TMIV (NR1aΔ5) also produced no detectable functional channels with NR2A. Since NR1aΔ4 forms a functional glycine binding site, these results show that the amino acid sequence before residue 380 is important for the formation of functional NMDA receptors.

TABLE I
*Electrophysiology data from Xenopus oocytes and HEK-293 cells co-expressing the NR1a truncations with NR2A*

Electrophysiological assays using 10 μM glutamate + 10 μM glycine were carried out in *Xenopus* oocytes injected with the indicated NR1a constructs and wild-type NR2A.

| | Current in *Xenopus* oocytes |
|---|---|
| | *pA* |
| NR1a + NR2A | 2107 ± 460 ($n$ = 13) |
| NR1aΔ1 + NR2A | 598 ± 272 ($n$ = 6) |
| NR1aΔ2 + NR2A | 209 ± 37 ($n$ = 7) |
| NR1aΔ3 + NR2A | 472 ± 149 ($n$ = 6) |
| NR1aΔ4 + NR2A | 0 ($n$ = 9) |
| NR1aΔ5 + NR2A | 0 ($n$ = 9) |

*Cell Surface Expression of NR2A When Co-expressed with the NR1a Truncations*—Cell surface expression of the NR2A subunit was determined by cell surface biotinylation following co-expression with the NR1a truncations. As reported previously (1), co-expression of NR1a and NR2A resulted in a streptavidin-isolated 180-kDa immunoreactive band, which was absent when NR2A was expressed alone (Fig. 2*A*). Progressive deletions to the N-terminal domain of NR1a led to a progressive decrease in the cell surface expression of NR2A until, with NR1aΔ4, there was no detectable surface NR2A (Fig. 2*B*). Similarly, no detectable levels of cell surface NR2A were found when the subunit was co-expressed with NR1aΔ7 and NR1aΔ8 (data not shown). Strikingly, the presence of a complete N terminus but deleted C terminus and TMIV of NR1a (NR1aΔ1 and NR1aΔ5, respectively) did not affect cell surface expression of NR2A (Fig. 2*C*). It should be noted that generally the levels of immunoreactive NR1a, the NR1a truncations, and NR2A were comparable in the cell lysates (Fig. 2, *B* and *C*, lysates). It is unlikely, therefore, that the differences in the surface expression of the constructs reflects differing levels of expression of the proteins. With the exception of NR1aΔ5, the cell surface expression data are in good agreement with the functional channel data, which suggests that the subunits can assemble to form functional channels provided the deletions in the N terminus of NR1a occur before residue 380. The lack of ion channel formation following expression of NR1aΔ5 with NR2A must therefore reflect some other effect of the loss of TMIV from the NR1a subunit, since this truncation does give rise to surface expression of NR2A.

*Effects of NR1 Truncations on Subunit Association Using Co-immunoprecipitation*—Since cell surface expression of NR2A might reflect both subunit association and oligomerization, co-immunoprecipitation studies were performed to determine the level of association of NR2A with the different NR1a

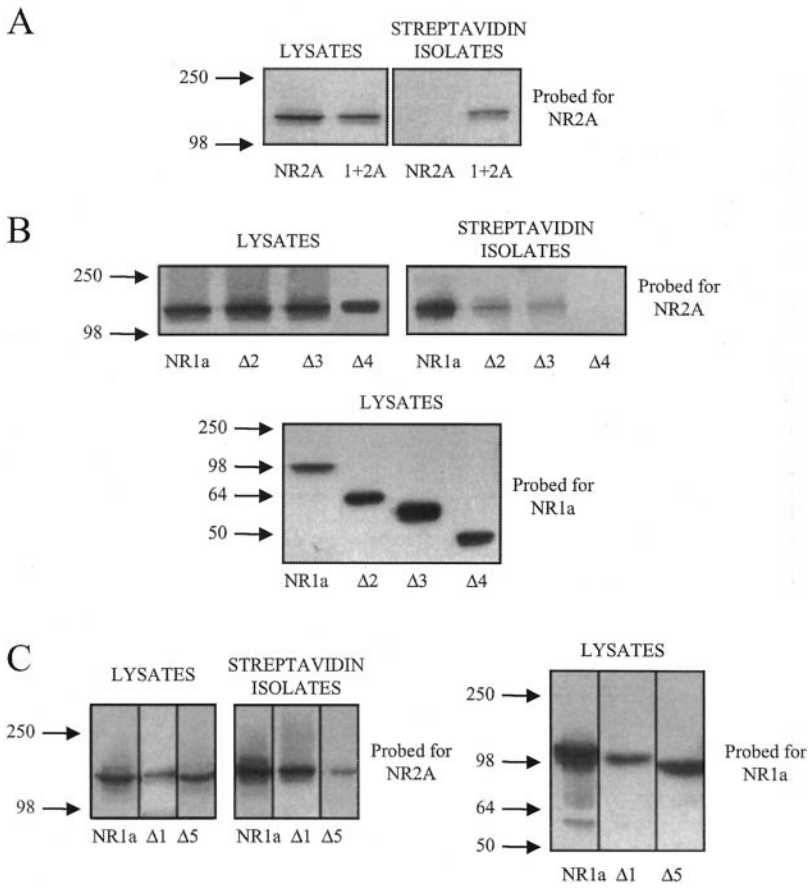


FIG. 2. **Cell surface expression of NR2A in HEK-293 cells when co-transfected with either NR1a or NR1a truncations.** *A*, HEK-293 cells were transiently transfected with NR2A alone or NR1a and NR2A and the cell surface expression of NR2A analyzed by biotinylation as described under "Experimental Procedures." *B*, HEK-293 cells were transiently transfected with NR2A and either NR1a or the indicated N-terminal truncations of NR1a. *C*, HEK-293 cells were transiently transfected with NR2A and either NR1a or the indicated C-terminal truncations of NR1a and the cell surface expression of NR2A determined as above. The cell lysates were also analyzed for the expression of the NR1a truncations using the NMDAR1 antibody. In this and all subsequent figures, the molecular sizes are given in kDa. The experiment was performed four times with comparable results.

truncations. The results showed that truncation of NR1a at the C terminus had no effect on the association of the subunits as illustrated for NR1aΔ5 (Fig. 3*A*). However, truncation of the N terminus resulted in a progressive loss of co-immunoprecipitating NR2A, which was barely detectable with NR1aΔ7 or NR1aΔ8 (Fig. 3*B*). Thus, there appears to be some residual association of NR1aΔ4 with NR2A, although this subunit does not give rise to either functional channels or surface expression of NR2A when the subunits are expressed together.

The results above could be interpreted as suggesting that the N-terminal region of NR1a from residues 1–380 are critical for subunit association. To test if they are sufficient for this, we have expressed NR2A with NR1a truncated just after the putative re-entrant loop of the second membrane domain and a chimera of NR1 where the N terminus of NR1a replaces that of GluR1 (Fig. 1). Co-expression of the NR1 truncation and NR1-GluR1 chimera with NR2A in HEK-293 cells did not give rise to cell surface expression (Fig. 4*A*), nor did they co-immunoprecipitate with NR2A (Fig. 4*B*). This suggests that residual precipitation seen when NR1aΔ4 and NR2A are co-expressed (Fig. 3*B*) is unlikely to be nonspecific and could suggest that the NR1a N-terminal alone may not be sufficient for association with NR2A.

*Oligomerization of the NMDA Receptor Complex*—The BN-PAGE described by Schagger *et al.* (31, 32) was adapted to provide a method for the determination of NMDA receptor subunit assembly. In the course of these studies, the BN-PAGE system has also been used to investigate nAChR oligomerization and the domains that are important in glycine receptor assembly (33, 34).

When BN-PAGE is used to analyze membranes derived from HEK-293 cells expressing the NR1a subunit alone, immunoreactive bands with apparent molecular masses of 200 and 420 kDa can be detected (Fig. 5*A*). The amount of the 200-kDa NR1a-immunoreactive band detected was variable and could reflect the different expression levels of the subunits in the different membrane preparations. When NR2A was co-expressed with NR1a, the molecular mass of the major NR1a immunoreactive species always shifted to give a broad band with a mean molecular mass of 860 kDa, with two additional immunoreactive bands at 420 and 200 kDa. Consistently, NR2A immunoreactivity could also be detected in the 860-kDa band but was not detected in the 200-kDa NR1a immunoreactive band (Fig. 5*A*). However, NR2A could also be detected in an immunoreactive band with a molecular mass of ~420 kDa when the 23.F6 antibody is used for detection, probably reflecting the greater sensitivity of this antibody compared with the anti-FLAG antibody. The intensity of this band, like that of the NR1a 200-kDa band, could be variable. The expression of the NR2A subunit alone in HEK-293 membranes resulted in streaking of the immunoreactive material, suggesting that the NR2A subunit might not be folding properly in the absence of NR1a (Fig. 5*A*, *right panel*).

Because the molecular sizes of the other receptor complexes analyzed by BN-PAGE have been reported to be larger than expected, the modified gel system used here for the NMDA receptors was used to analyze $GABA_A$ receptors and *Torpedo* nAChR of known stoichiometry (32, 35). Under BN-PAGE conditions, the $GABA_A$ receptor migrated with an apparent molecular mass of 540 kDa, about twice that predicted from its known subunit composition (Fig. 5*B*). The nAChR complex in these gels had an apparent molecular mass of 400 kDa, which is ~150 kDa larger than the predicted 250-kDa pentamer (Fig. 5*B*). Another immunoreactive band was also detected migrating with an apparent molecular mass of 660 kDa, which may represent a dimer of the pentameric nAChR complex formed through a disulfide bridge between the δ subunits. Denaturation of the nAChR complex using 0.1 M dithiothreitol and 8 M

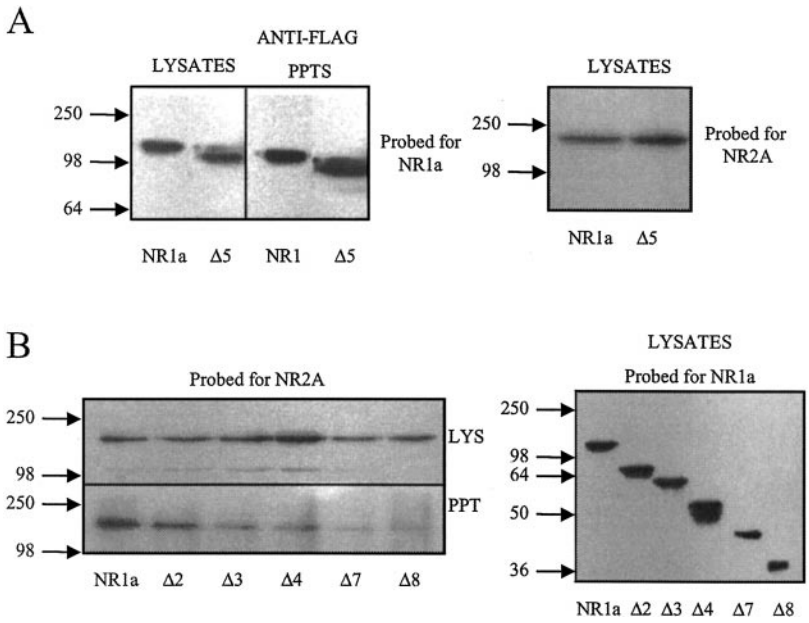


FIG. 3. **Co-immunoprecipitation from HEK-293 cell lysates of the NR2A subunit co-expressed with the NR1 truncations.** HEK-293 cells co-expressing FLAG epitope-tagged NR2A and the NR1a C-terminal truncation NR1a Δ5 (*A*) and the indicated NR1a N-terminal truncations containing a full-length C terminus (*B*) were processed for immunoprecipitation as described under "Experimental Procedures" using anti-FLAG antibody (*A*) or NR1a C-terminal antibody (*B*). NR1a N-terminal truncations containing a full-length C terminus were used in this experiment to allow all the immunoprecipitations of the NR1a N-terminal truncations to be performed using the same antibody, namely that raised against the NR1a C terminus. All the lysates (*LYS*) and immunoprecipitates (*PPTS*) were probed for NR2A using the C-terminal anti-NR2A serum, and the NR1 subunits detected in both the cell lysates and immunoprecipitates using the anti-NR1a C-terminal antibody. The experiment was performed seven times with comparable results.

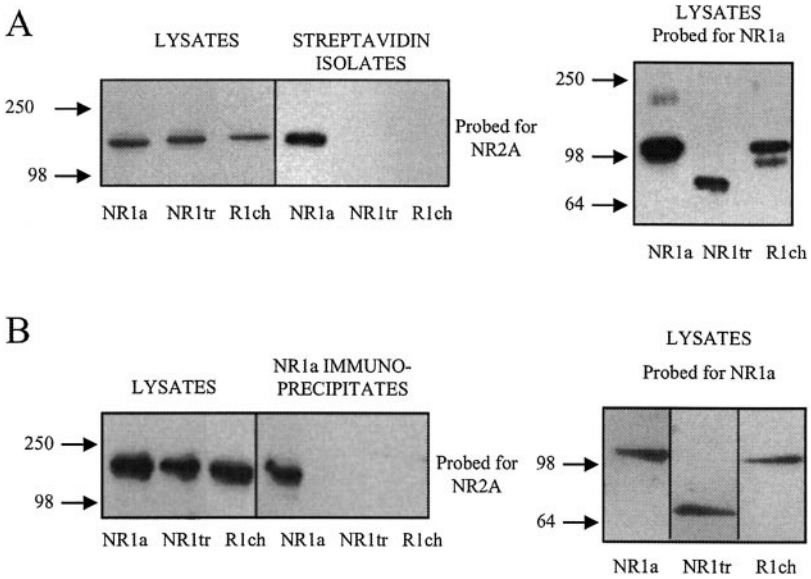


FIG. 4. **The N terminus of NR1a is not sufficient for subunit association.** NR2A was co-expressed with the NR1a, N-terminal truncations of NR1a (*NR1tr*), and the NR1-GluR1 chimera (*R1ch*) in HEK-293 cells. The surface expression of NR2A was determined by cell surface biotinylation (*A*) and subunit association with NR2A determined by co-immunoprecipitation (*B*). Immunoprecipitation was performed using the anti-FLAG antibody or anti-GluR1 antibody. The presence of the NR1a subunits in all the cell lysates were determined using the NR1a N terminus antibody. The experiment was performed four times with comparable results.

urea, as described previously (35), led to the detection of several lower order intermediates, suggesting the stoichiometry of the 400-kDa nAChR complex detected by BN-PAGE was indeed pentameric (data not shown).

Analysis of the oligomerization of the NR1a N-terminal deletion constructs co-expressed with NR2A resulted in diffuse regions of immunoreactive material within which some discrete banding for the NR1a constructs and NR2A could still be seen when the immunoblots were probed for either NR1a and NR2A (Fig. 6*A*). This suggests that deletions in the N terminus of the NR1a subunit may cause incomplete or misfolding of the subunits, although some association of the subunits may still occur. This is in agreement with the surface expression and functional data. Expression of the C-terminal truncations of NR1a (NR1aΔ1 and NR1aΔ5) with NR2A did not affect the appearance of a large molecular weight immunocomplex containing both NR1a and NR2A, following analysis of the membranes by BN-PAGE (Fig. 6*B*), although the complex was reduced in size due to the deletions. Both NR1aΔ1 and NR1aΔ5 gave rise to immunoreactive bands at positions lower on the gel, corresponding to the 420-kDa band for NR1a. Interestingly, when probed for NR2A, a slower migrating immunoreactive band at this position is also present in the gels, which suggests that this is a dimer containing the two subunits. When NR1aΔ1 and NR1aΔ5 were expressed alone, they yielded immunoreactive bands on BN-PAGE similar to those seen with the full NR1a subunit (200 and 420 kDa), although with the expected reduction in molecular sizes (data not shown). These results show that the oligomerization of the subunits is not affected by the C-terminal deletions and explains why they give rise to full surface expression of NR2A.

*Characterization of the Oligomerization of the NMDA Receptor Using Sucrose Gradient Density Centrifugation*—In order to confirm whether the BN-PAGE system was giving a reliable indication of NR1a and NR2A association, the assembly of the subunits was also examined by sucrose gradient centrifugation. Immunoblots of the gradient fractions from HEK-293 cell lysates expressing either the NR1a or NR2A subunit alone show that NR1a has a lower sedimentation rate than NR2A (Fig. 7*A*). The NR1a subunit sediments close to the aldolase marker (150 kDa/7.3 *s*), which may suggest that the NR1a subunit is a dimer, as seen in the BN-PAGE analysis. The NR2A subunit has a more heterodisperse sedimentation profile, with a significant amount of NR2A at the bottom of the gradient (Fig. 7*A*).

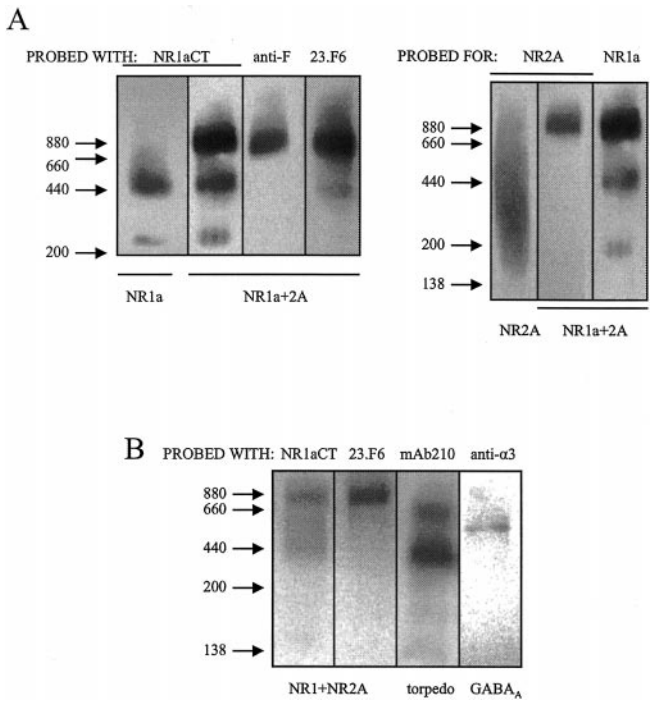


FIG. 5. **Characterization of the oligomerization of the NR1a subunit and the wild-type NMDA receptor complex using BN-PAGE.** *A*, HEK-293 membranes co-expressing NR1a, NR2AFLAG, or both subunits were analyzed using BN-PAGE. The resulting immunoblots were probed with NR1a C-terminal antibody (*NR1aCT*), anti-FLAG antibody (*anti-F*), and the 23.F6 antibody. *B*, cell membranes expressing NR1a or NR1a/NR2A subunits, GABA ($\alpha_3\beta_3\gamma_2$) subunits, and purified *Torpedo* nAChR protein were analyzed using BN-PAGE. The resulting immunoblot was probed with NR1aCT, 23.F6, anti-α3, and monoclonal antibody (*mAb*) 210. The experiment was performed three times with comparable results.

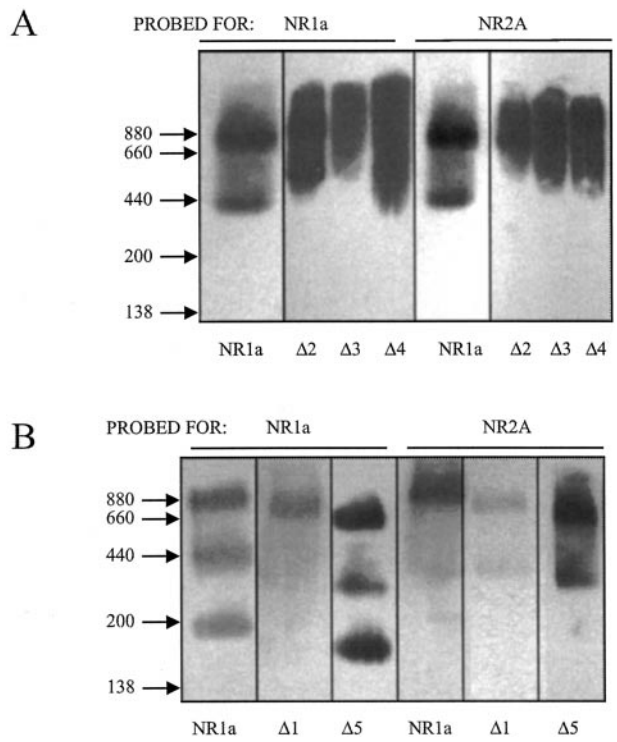


FIG. 6. **Characterization of the oligomerization of the NR1a truncations co-expressed with NR2A by BN-PAGE.** Membranes from HEK-293 cells co-expressing NR2A with the indicated NR1a N-terminal truncations (*A*) or C-terminal truncations (*B*) were analyzed using BN-PAGE. The resulting immunoblots were probed with the NMDAR1 and the 23.F6 antibodies. The experiment was performed five times with comparable results.

The smearing of NR2A across the gradient and the insoluble material pelleting at the bottom of the gradient suggests that the NR2A subunit may not fold properly when it is expressed alone, supporting the data obtained from the BN-PAGE system. When cell lysates from HEK-293 cells co-expressing NR1a and NR2A subunits were analyzed on sucrose gradients, two peaks of immunoreactivity for NR1a were detected. One peak was detected in the same fraction as the aldolase marker (150 kDa/7.3 *s*), and the second peak was found further down the gradient in the fractions below the catalase marker (230 kDa/11 *s*; Fig. 7*B*). This peak also contained the majority of the NR2A immunoreactivity, which was now contained in a more discrete region of the gradient. Together, the data suggest that the NR1a and NR2A subunits are assembling to form a complex that is not present when either NR1a or NR2A subunits are expressed alone. Thus, the BN-PAGE analysis of receptor oligomerization was supported by the sucrose gradient analysis.

*Identifying the Molecular Determinants Important in the Assembly of NMDA Receptor Complexes Using Secreted Soluble Forms of the NR1a Subunit*—The importance of the NR1a subunit transmembrane domains for subunit association with NR2A was studied using soluble constructs of the NR1a subunit. The S1S2-SHORT construct consists of the S1 and S2 domains of NR1a linked by a flexible linker sequence (Fig. 1). The S1S2-LONG construct has the full N-terminal domain of NR1a linked to the S2 domain in the same manner as S1S2-SHORT. Expression of these constructs in HEK-293 cells results in a soluble secreted form of the proteins being found in the medium from the cells (Fig. 8*A*).

Analysis of the secreted product from S1S2-SHORT transfected cells by size exclusion chromatography and SDS-PAGE shows two peaks of immunoreactivity: one eluting just before the 45-kDa ovalbumin marker fraction and a major broad peak, which included the void fraction. The latter probably represents aggregated protein whereas the former corresponds to a monomer of the S1S2 protein (Fig. 8*B*). A similar analysis of S1S2-LONG secreted material showed that this construct also elutes as two peaks of immunoreactivity: one eluting just behind the void fraction and the major peak eluting just before the IgG marker of 150 kDa (Fig. 8*B*). As the monomeric form of the S1S2-LONG construct has an apparent molecular mass of 98 kDa, the data suggest that the S1S2 construct containing a complete N-terminal domain can dimerize. This lends credence to the homo-oligomerization of the NR1a subunit detected using BN-PAGE.

*Cell Surface Expression of NR2A Co-expressed with the S1S2-SHORT and S1S2-LONG Constructs*—S1S2-LONG and S1S2-SHORT were co-expressed in HEK-293 cells with NR2A and cell surface biotinylation used to monitor NR2A cell surface expression. NR2A could only be detected at the cell surface when co-expressed with the S1S2 construct that contained a complete N-terminal domain (Fig. 9). S1S2-LONG but not S1S2-SHORT could also be detected in the streptavidin isolates (Fig. 9).

## DISCUSSION

In this study we have used the surface expression of NR2A when co-expressed with different NR1a truncations to determine the regions of NR1a that are important for subunit association and oligomerization. Deletions from the C terminus of NR1a up to residue 811 had no effect on the surface expression of NR2A, whereas deletion between residues 312–380 at the N terminus of NR1a (NR1aΔ4) prevented cell surface expression of NR2A. The progressive loss of surface expression of NR2A

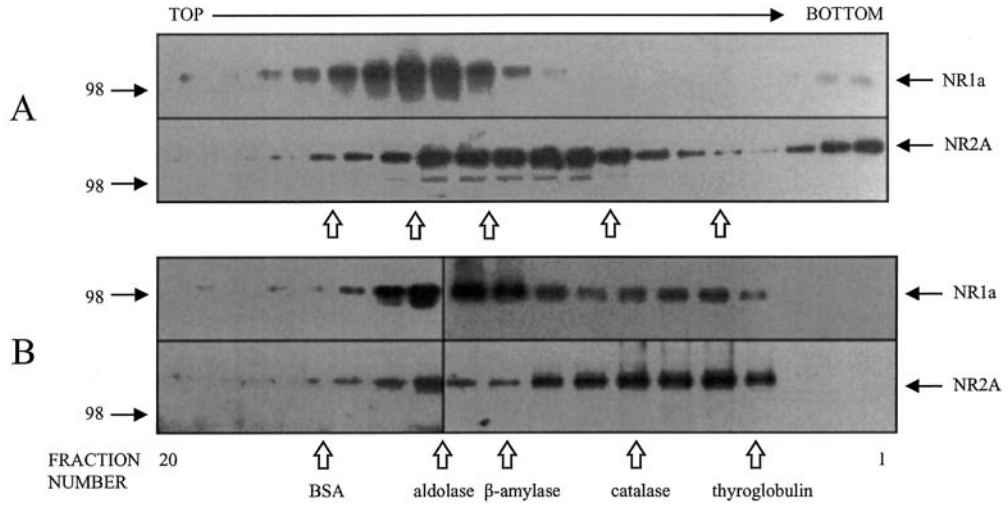


FIG. 7. **SDS-PAGE of sucrose gradient fractions from HEK-293 cells expressing NR1a or NR2A subunits.** HEK-293 cells expressing either NR1a or NR2A subunits alone (*A*) or together (*B*) were lysed in 1% Triton X-100 and analyzed by sucrose gradient centrifugation and SDS-PAGE. The resulting immunoblots were probed with either the NMDAR1 antibody (*A*) or the NR2A C-terminal antibody (*B*). The position of the marker proteins on the gradient is indicated by the *arrows*. These were bovine serum albumin (*BSA*, 66 kDa; 4.4 *s*), aldolase (150 kDa; 7.3 *s*), β-amylase (200 kDa; 8.9 *s*), catalase (230 kDa; 11 *s*), and thyroglobulin (660 kDa; 19.2 *s*).

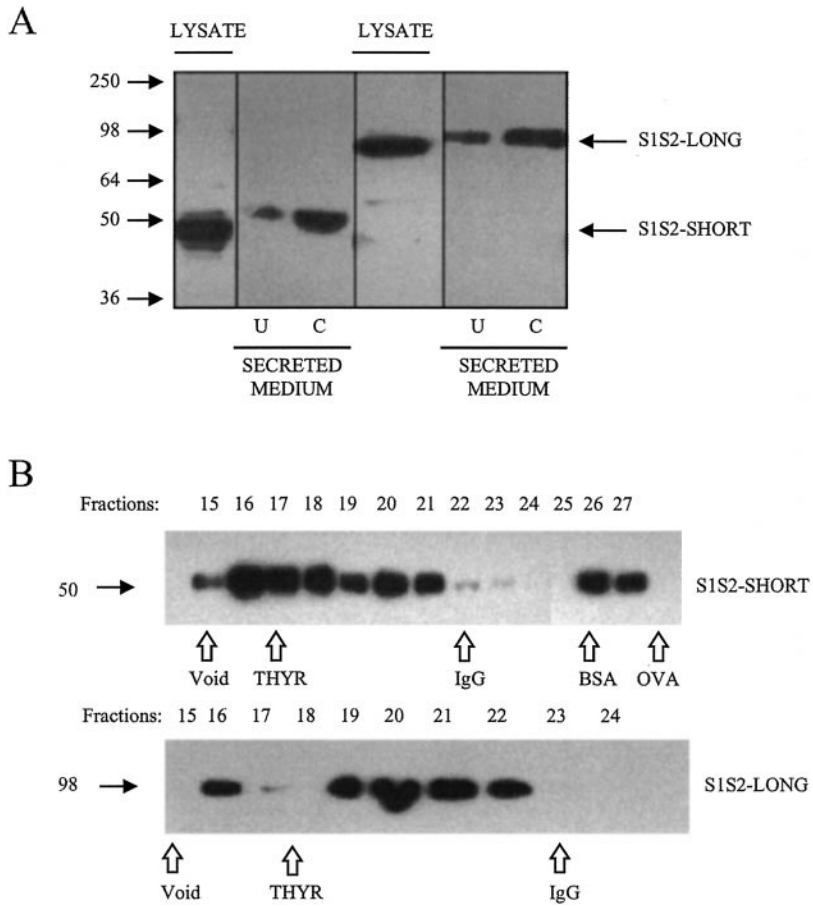


FIG. 8. **Characterization of the proteins produced by the S1S2-SHORT and S1S2-LONG constructs transfected into HEK-293 cells.** HEK-293 cells were transfected with S1S2-SHORT and LONG constructs, and after 48 h the cells were harvested and total cell lysates formed and the supernatant concentrated. Samples were analyzed using SDS-PAGE and the resulting immunoblot probed with the NMDAR1 antibody (*A*). The SHORT and LONG constructs had apparent molecular masses of ~50 and 98 kDa, respectively, and were found in the cell culture medium. *U*, unconcentrated media; *C*, concentrated media. *B*, concentrated medium was analyzed by size exclusion chromatography and the fractions analyzed by SDS-PAGE and Western immunoblot. The elution position of the molecular size standards are shown: ovalbumin (*OVA*; 45 kDa), bovine serum albumin (*BSA*; 66 kDa), immunoglobulin G (*IgG*; 150 kDa), and thyroglobulin (*THYR*: 660 kDa).

with increasing truncation of NR1a N terminus suggests a progressive effect on the association of the two subunits (Fig. 3). Electrophysiological studies support the conclusions based on cell surface expression of NR2A, as the NR1a N-terminal truncations with deletions up to residue 312 showed reduced currents following agonist exposure compared with the full-length subunit. Deletions between residues 312 and 380 of the NR1a subunit resulted in no functional channels (Table I). The data from the BN-PAGE analysis of the NR1a N-terminal truncations suggest they are misfolding or folding incompletely (Fig. 6*A*). It seems unlikely that this possible misfolding alone explains the lack of subunit association, since all of the NR1a N-terminal truncations give rise to high affinity glycine antagonist binding sites and, with the exception of NR1aΔ4, functional channels. However, it is highly probable that the integrity of the LIVPB domain of NR1a (residues 1–380) may contribute to the proper folding of the NR1a subunit. In this context we note that it has been described that deletions of the GluR4 subunit at the N terminus causes disruption of subunit folding when these mutants are expressed in mammalian cells

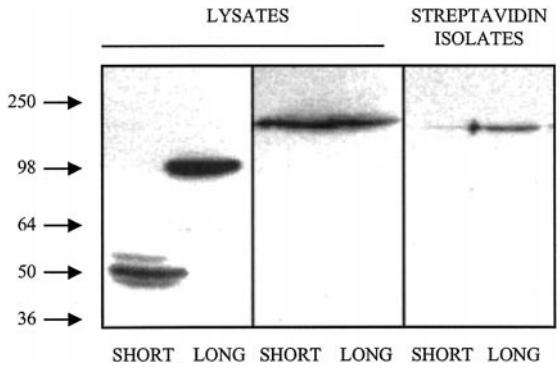


FIG. 9. **Cell surface expression of NR2A in HEK-293 cells when co-expressed either the S1S2-SHORT or the S1S2-LONG constructs.** Cell surface expression of NR2A co-expressed with S1S2-SHORT and S1S2-LONG constructs in HEK-293 cells was analyzed by cell surface biotinylation. Samples of the total cell lysates and streptavidin isolates of membrane proteins were analyzed using SDS-PAGE. The resulting immunoblot of total cell lysates and streptavidin isolates was overlaid, with the NR2A C-terminal antibody and the cell lysates also probed for the presence of the constructs with the NMDAR1 antibody. The experiment was performed three times with comparable results.

(36). Therefore, the N-terminal domain of NR1a (between residues 1–380) seems to be critical for the association with NR2A. However, the data obtained from the NR1a truncated N terminus and NR1-GluR1 chimera appear to suggest that the N-terminal region alone of NR1a alone may not be sufficient to give cell surface expression of NR2A and may therefore not be sufficient for subunit association (Fig. 4).

Failure of cell surface expression of NR2A when co-expressed with the NR1a truncations, observed with cell surface biotinylation, could be explained in several ways. It could represent a failure of the subunits to associate, a failure of oligomerization, or formation of unstable associations and/or oligomers between the NR1a and NR2A subunits. Therefore, the association of NR1a with NR2A using co-immunoprecipitation was determined. The results showed that progressive deletions to the N-terminal domain of NR1a caused a reduction in the amount of NR2A that could be co-immunoprecipitated (Fig. 3). Deletions after residue 380 appeared to almost completely abolish the association of NR2A with NR1a, suggesting that residues before this are important for NR1a/NR2A association. Since we found residual co-immunoprecipitation of NR2A when co-expressed with NR1aΔ4 but not when co-expressed with the NR1 N-terminal truncation or NR1-GluR1 chimera (Fig. 4), we cannot exclude the possibility that residues following 380 may contribute, in part, to subunit association such as the S2 domain. However, it is clear that residues 1–380 are critical for NMDA receptor subunit association and oligomerization, similar to the findings in the AMPA receptor by Leuschner *et al.* (27).

Since cell surface expression may also reflect subunit oligomerization, the assembly status of the subunits was assessed using BN-PAGE. This methodology permitted the analysis of the oligomerization of the NMDA receptor since a band of ~860 kDa, which was immunoreactive for both NR1a and NR2A, only appeared when using membranes from HEK-293 cells co-transfected with both NR1a and NR2A subunits. The size of this complex is similar to that found by analyses of the NMDA receptor complex in previous reports (14–16). To address the issue of receptor stoichiometry using the BN-PAGE system, we used this technique to investigate the stoichiometry of the nAChR and the $GABA_A$ receptor (Fig. 5). We observed that the BN-PAGE system gives larger molecular sizes for the receptors than has been elucidated previously, which is consistent with other reports (35). The increased molecular weight of these receptors suggests that detergent and/or Coomassie Blue binding affects the masses of receptor complexes under the gel conditions, making it difficult to determine receptor subunit stoichiometry from these gels. However, by comparing the molecular masses of the $GABA_A$ receptor and the nAChR with those obtained by the BN-PAGE system used here, it appears that there is consistent overestimate of receptor mass by between 1.6- and 1.8-fold. If a similar effect was operating on the NMDA receptor subunits, then the revised molecular masses seen for the NR1a immunoreactive bands, when the subunit is expressed alone, would be in the range of 100–117 kDa and 200–247 kDa, which would suggest a monomer and dimer of the subunit. Similarly, the immunoreactive bands seen when NR1a and NR2A are co-expressed would be 440–517 kDa and 200–247 kDa, consistent with a tetramer of two NR1 and two NR2A subunits and a dimer of NR1a and NR2A, respectively. However, the broad nature of the bands and the compression of the molecular weight markers on these gels at the higher molecular weights prevent a precise attribution of stoichiometry for the full receptor. Nevertheless, the fact that the NR1a and NR2A immunoreactivity undergoes such a dramatic redistribution when the subunits are expressed together suggests that these gels do allow the oligomerization of the NMDA receptor to be investigated.

It seems likely that the oligomeric NR1a bands formed when the subunit is expressed alone do represent the monomer and dimer of NR1a. Not only would this fit with the estimated molecular weight, but it is consistent with the sucrose gradient and S1S2-LONG data, which also suggest that NR1a can form homodimers (Fig. 8*B*). Together these data suggest that the NR1a subunit can self-associate to form higher oligomers, as suggested by other studies of soluble NR1 and AMPA receptor subunits (37, 38). Surprisingly the BN-PAGE system also showed that NR2A may not be folding properly when expressed alone, suggesting that this subunit may not form homo-oligomers like the NR1a subunit (Fig. 5). This is also consistent with the sucrose gradient analyses of HEK-293 cell lysates expressing NR2A alone (Fig. 7).

The NR1a truncations with deleted C terminus and TMIV (NR1aΔ1 and NR1aΔ5) were able to co-assemble with NR2A (Fig. 3) and oligomerize into a complex present at the cell surface similar to that seen with the wild-type NR1a and NR2A subunits (Figs. 2, 5, and 6). However, deletion of the C terminus and TMIV of NR1a (NR1aΔ5) led to formation of a nonfunctional complex with NR2A in our electrophysiological studies (Table I). Thus, TMIV of the NR1a subunit is critical for formation of functional NMDA receptor channels, but deletion of the C-terminal tail and TMIV of NR1a does not affect NMDA receptor subunit association or oligomerization. Interestingly, it has been suggested that TMIV of iGluR subunits is positioned away from the channel pore but interacts with the pore-forming TMI and TMIII domains to form a functional channel (39).

The role of the transmembrane domains in facilitating the assembly of the NMDA receptor was examined using soluble NR1a S1S2 domains, either with (S1S2-LONG) or without (S1S2-SHORT) the LIVBP domain, similar to those described in earlier studies on both AMPA and NR1 subunits (38, 40–42). The resulting constructs were expressed in HEK-293 cells and the cell lysate and culture medium analyzed for the presence of the proteins (Fig. 8*A*). Immunoblots of the secreted constructs revealed immunoreactive bands with apparent molecular masses of 50 and 98 kDa detected in the S1S2-SHORT and S1S2-LONG cell lysates and supernatants, respectively. These molecular sizes are consistent with the predicted molecular size of the proteins produced from the S1S2 constructs.

The BN-PAGE method of analyzing the oligomerization of receptor subunits yielded only heterodisperse bands of concentrated media containing the secreted S1S2 constructs (data not shown), so size exclusion chromatography was used as an alternative method to analyze the soluble NR1a constructs (Fig. 8*B*). The majority of S1S2-SHORT eluted in the void fraction, with some material eluting with an apparent molecular mass of 45 kDa. This suggests that the S1S2-SHORT construct produces protein, which is forming large aggregates with only a proportion of the secreted protein eluting as a discrete peak with the predicted mass of 45 kDa. Other studies investigating the oligomerization of soluble S1S2 domains of other glutamate receptor subunits have also found that the soluble short forms of the S1S2 domains remain as monomers in solution (40, 43, 44). However, using a soluble domain of the NMDA receptor similar to the S1S2 short construct described here, Ivanovic *et al.* (38) found that the secreted protein formed large aggregates as well as what appeared to be a dimer. The differences in the hydrodynamic properties of their secreted protein and that described here might reflect the fact that we have expressed our protein in mammalian cells rather than in insect cells.

The S1S2-LONG construct produced a protein that eluted with a molecular mass of 200 kDa, which suggests the formation of a dimer of the 98-kDa polypeptide. Studies using other glutamate receptor subunit S1S2 constructs with a complete extracellular N-terminal domain have also detected complexes with molecular weights similar to that predicted for a dimer (40). Therefore, the data obtained from the NR1 S1S2-SHORT and S1S2-LONG constructs are consistent with these findings and show that the NR1a subunit can form a homodimer, which is dependent on the presence of the intact LIVBP domain.

Interestingly, only the S1S2 construct that formed homodimers (S1S2-LONG) could assemble with NR2A, as demonstrated in our cell surface biotinylation studies (Fig. 9). This indicates the importance of dimerization of the NR1a subunit, as well as the presence of a complete N-terminal domain, for stable assembly with NR2A. The fact that S1S2-LONG can cause surface expression of NR2A suggests that the transmembrane domains of NR1a are not essential for subunit association, although our data do not rule out that they may be important for either higher oligomerization of the subunits or for stable subunit association.

In conclusion the data presented here show that the LIVBP domain of NR1a (residues 1–380) make a significant contribution toward the self-association of the subunit as well as its interaction with NR2A. However, the N-terminal domain of NR1a alone may not be sufficient for its association with NR2A. In addition, the NR1a transmembrane domains are not essential for association with NR2A, nor are the NR1a C terminus or TMIV. This study also finds that deletions in the N terminus of NR1a may affect its folding, and that NR2A may not fold efficiently in the absence of NR1, which has clear implications for the design of studies aimed at defining more closely the regions of these subunits that are critical for subunit interaction.

REFERENCES


1. McIlhinney, R. A. J., Le Bourdellès, B., Tricuad, N., Molnar, E., Streit, P., and Whiting, P. J. (1998) *Neuropharmacology* **37,** 1355–1367
2. Dingledine, R., Borges, K., Bowie, D., and Traynelis, S. F. (1999) *Pharmacol. Rev.* **51,** 7–61
3. Cik, M., Chazot, P. L., and Stephenson, F. A. (1993) *Biochem. J.* **296,** 877–883
4. Grimwood, S., Le Bourdelles, B., and Whiting, P. J. (1995) *J. Neurochem.* **64,** 525–530
5. Varney, M. A., Jachec, C., and Deal, C. (1996) *J. Pharmacol. Exp. Ther.* **279,** 367–378
6. Kuryatov, A., Laube, B., Betz, H., and Kuhse, J. (1994) *Neuron* **12,** 1291–1300
7. Wafford, K. A., Kathoria, M., Bain, C. J., Marshall, G., Le Bourdelles, B., Kemp, J., and Whiting, P. J. (1995) *Mol. Pharmacol.* **47,** 374–380
8. Hirai, H., Kirsch, J., Laube, B., Betz, H., and Kuhse, J. (1996) *Proc. Natl. Acad. Sci. U. S. A.* **93,** 6031–6036
9. Laube, B., Hirai, H., Sturgess, M., Betz, H., and Kushe, J. (1997) *Neuron* **18,** 493–503
10. Anson, L. C., Chen, P. E., Wyllie, D. J. A., Colquhoun, D., and Schoepfer, R. (1998) *J. Neurosci.* **18,** 581–589
11. Patneau, D. K., and Mayer, M. L. (1990) *J. Neurosci.* **10,** 2385–2399
12. Benveniste, M., and Mayer, M. L. (1991) *Br. J. Pharmacol.* **104,** 207–221
13. Clements, J. D., and Westbrook, G. L. (1991) *Neuron* **7,** 605–613
14. Blahos, J., and Wenthold, R. J. (1996) *J. Biol. Chem.* **271,** 15669–15674
15. Brose, N., Gasic, G. P., Vetter, D. E., Sullivan, J. M., and Heinemann, S. F. (1993) *J. Biol. Chem.* **268,** 22663–22671
16. Chazot, P. L., Coleman, S. K., Cik, M., and Stephenson, F. A. (1994) *J. Biol. Chem.* **269,** 24403–24409
17. Hawkins, L., Chazot, P., and Stephenson, F. A. (1999) *J. Biol. Chem.* **274,** 27211–27218
18. Behe, P., Stern, P., Wylie, D. J. A., Nassar, M., Schoepfer, R., and Colquhoun, D. (1995) *Proc. R. Soc. Lond. Ser. B Biol. Sci.* **262,** 205–213
19. Laube, B., Kuhse, J., and Betz, H. (1998) *J. Neurosci.* **18,** 2954–2961
20. Premkumar, L. S., and Auerbach, A. (1997) *J. Gen. Physiol.* **110,** 485–502
21. Bennett, J. A., and Dingledine, R. (1995) *Neuron* **14,** 373–384
22. Hollmann, M. (1997) *The Ionotropic Glutamate Receptors*, pp. 3–98, Humana Press, New York
23. Wo, Z. G., and Oswald, R. E. (1994) *Proc. Natl. Acad. Sci. U. S. A.* **91,** 7154–7158
24. Lampinen, M., Pentikainen, O., Johnson, M. S., and Keinanen, K. (1998) *EMBO J.* **17,** 4704–4711
25. Sternbach, Y., Bettler, B., Hartley, M., Sheppard, P. O., O'Hara, P. J., and Heinemann, S. F. (1994) *Neuron* **13,** 1345–1357
26. Ferns, M., Hoch, W., Campanelli, J. T., Rupp, F., Hall, Z. W., and Scheller, R. H. (1992) *Neuron* **8,** 1079–1086
27. Leuschner, W. D., and Hoch, W. (1999) *J. Biol. Chem.* **274,** 16907–16916
28. Sandhu, S., Grimwood, S., Mortshire-Smith, R. J., Whiting, P. J., and Le Bourdelles, B. (1999) *J. Neurochem.* **72,** 1694–1698
29. Robbins, M. J., Ciruela, F., Rhodes, A., and, McIlhinney R. A. J. (1999) *J. Neurochem.* **72,** 2539–2547
30. Molnar, E., McIlhinney, R. A. J., Baude, A., Nusser, Z., and Somogyi, P. (1994) *J. Neurochem.* **63,** 683–693
31. Schagger, H., and von Jagow, G. (1991) *Anal. Biochem.* **199,** 220–231
32. Schagger, H., Cramer, W. A., and von Jagow, G. (1994) *Anal. Biochem.* **217,** 220–230
33. Nicke, A., Rettinger, J., Mutschler, E., and Schmalzing, G. (1999) *J. Recept. Signal Transduct. Res.* **19,** 493–507
34. Griffon, N., Buttner, C., Nicke, A., Kuhse, J., Schmalzing, G., and Betz, H. (1999) *EMBO J.* **18,** 4711–4721
35. Nicke, A., Baumert, H. G., Rettinger, J., Eichele, A., Lambrecht, G., Mutschler, E., and Schmalzing, G. (1998) *EMBO J.* **17,** 3016–3028
36. Coleman, S. K., and Keinanen, K. (2000) *Forum Eur. Neurosci. Proc.* **12,** 37
37. Kuusinen, A., Arvola, M., and Keinanen, K. (1995) *EMBO J.* **14,** 6327–6332
38. Ivanovic, A., Reilander, H., Laube, B., and Kuhse, J. (1998) *J. Biol. Chem.* **273,** 19933–19937
39. Sutcliffe, M. J., Galen Wo, Z., and Oswald, R. E. (1996) *Biophys. J.* **70,** 1575–1589
40. Kuusinen, A., Abele, R., Madden, D. R., and Keinanen, K. (1999) *J. Biol. Chem.* **274,** 28937–28943
41. Miyazaki, J., Nakanishi, S., and Jingami, H. (1999) *Biochem. J.* **340,** 687–692
42. Armstrong, N., Sun, Y., Chen, G.-Q., and Gouaux, E. (1998) *Nature* **395,** 913–917
43. Abele, R., Svergun, D., Keinanen, K., Koch, M. H. J., and Madden, D. R. (1999) *Biochemistry* **38,** 10949–10957
44. Chen, G.-Q., and Gouaux, E. (1997) *Proc. Natl. Acad. Sci. U. S. A.* **94,** 13431–13436